European Journal of Soil Science

*European Journal of Soil Science*, June 2011, **62**, 408–416 doi: 10.1111/j.1365-2389.2011.01366.x

# A geostatistical two-phase sampling strategy to map soil heavy metal concentrations in a former war zone

E. Meerschman, L. Cockx & M. Van Meirvenne

*Faculty of Bioscience Engineering, Department of Soil Management, Research Group Soil Spatial Inventory Techniques, Ghent University, Coupure 653, B-9000 Gent, Belgium*

## Summary

In a recent paper it was concluded that an enrichment of copper (Cu) content by 6 mg $kg^{-1}$ dry mass in the soil around Ypres (Belgium) was a legacy of shelling during the First World War. This conclusion was based on a regional database of the entire province of West-Flanders (3144 $km^2$) containing a limited number of soil samples in the war zone. Shells partly consisted of an alloy of Cu and zinc (Zn), and shrapnel balls were made out of lead (Pb). We expanded the database with a two-phase sampling design, each of 100 samples, in the war zone surrounding Ypres (640 $km^2$) to (i) increase the detail of the inventory and (ii) expand the database to include Cu, Pb and Zn. This article focuses on the geostatistical selection of additional sampling locations. As the enrichment was spatially continuous and our aim was to map accurately over the range of values, rather than to delineate the enriched area, conventional selection criteria based on the probability of exceeding a critical threshold were not suitable. Therefore the sampling locations were optimized using a combination of selection criteria based on the kriging variance, the conditional variance and the conditional coefficient of variation obtained with sequential Gaussian simulation. A jackknife validation with 102 independent observations indicated the improvement after each phase. Additionally, the local uncertainty maps tended to show reduced values and a more homogenous pattern as additional samples were added. In an overview of the final prediction maps for Cu, Pb and Zn it is clear that those for Cu and Pb reflect the position of the main front line.

## Introduction

In a study focusing on the occurrence of soil heavy metal concentrations in West-Flanders (Belgium), Van Meirvenne *et al.* (2008) concluded that the topsoil of the former war zone around Ypres was currently characterized by an average copper (Cu) enrichment of 6 mg $kg^{-1}$ soil (dry mass, DM), resulting from the millions of shells fired in the First World War (WWI). The enrichment can be seen as an increase in the geochemical baseline concentration and is spatially continuous, unlike a local point contamination.

However, this conclusion was based on a regional database of the entire province of West-Flanders (3144 $km^2$) with a limited number of soil samples located in the war zone. The Cu concentrations were interpolated for a prediction grid with a resolution of 500 m by 500 m. Furthermore, the chemical composition of the WWI ordnance consisted not only of a considerable amount of Cu, but zinc (Zn) was also used in the top fuse and the rotating band of a shell and shrapnel balls were made out of lead (Pb). Therefore, the Flemish government decided that extra samples were needed to improve the level of detail inside the enriched region, allowing interpolation on a prediction grid of 200 m by 200 m, and that data on Pb and Zn were also required. This paper describes the development of a multiphase geostatistical sampling strategy for a spatially continuous enrichment of heavy metals in soils, thereby taking into account budget and time constraints.

Although a multiphase sampling strategy based on geostatistical selection criteria has already proven its efficiency (Chien, 1998; Verstraete & Van Meirvenne, 2008), for every specific situation an optimization is needed with respect to the number of samples, the number of phases and the type of selection criterion. To increase the overall cost efficiency, the challenge is to determine for each sampling phase which selection criterion is the most appropriate given the available data, circumstances and gathered knowledge.

A commonly applied criterion in local point pollution studies is sampling at locations where the conditional probability of a variable $Z(\mathbf{x})$ (with $\mathbf{x}$ the vector of coordinates) exceeding a critical threshold $z_c$ is around 50% (Garcia & Froidevaux, 1997; Barabás *et al.*, 2001; D'Or, 2005; Pardo-Igúzquiza & Dowd, 2005;

Correspondence: E. Meerschman. E-mail: Eef.Meerschman@UGent.be

Received 15 October 2009; revised version accepted 28 February 2011

Verstraete & Van Meirvenne, 2008). This strategy allows an isarithm for the concentration that corresponds to this threshold to be accurately mapped, as is required for decisions on remediation. However, this criterion does not ensure that variations above or below the threshold are mapped precisely, whereas our aim is to map the heavy metal enrichment accurately over the range of values, rather than to delineate the enriched area. Moreover, determining a critical threshold is not straightforward in our case. Legal soil quality thresholds exist, but are not useful in the case of an increase of the baseline concentration, while the methods to define geochemical baseline concentrations are still under development (Meklit *et al*., 2009).An alternative is the design of a sampling scheme that minimizes the mean, or the maximum, ordinary kriging variance ($\sigma^2_{OK}$) (Webster & Burgess, 1984; Van Groenigen & Stein, 1998). This prediction error variance is conditional on the variogram and the configuration of the data points and independent of the data values, allowing the user to predict the impact of the sampling campaign on $\sigma^2_{OK}$ beforehand (Burgess *et al*., 1981; Englund & Heravi, 1994).

In contrast to the kriging variance, the conditional variance ($\sigma^2_C$), determined by the conditional cumulative distribution function (ccdf), not only depends on the data configuration but also on the data values (Goovaerts, 1997). Lloyd & Atkinson (1999) demonstrated that maps of the conditional variance are appropriate for sampling of data to improve existing datasets. Because of the heteroscedasticity of $\sigma^2_C$, locations with the largest $\sigma^2_C$ are found in areas where large concentrations are predicted (Van Meirvenne & Goovaerts, 2001). These authors proposed the use of conditional coefficient of variation ($CV_C$). Whereas $\sigma^2_C$ can be seen as a measure of the absolute uncertainty, the relative uncertainty can be expressed by $CV_C$. As each selection criterion has its own characteristics, it is advantageous to combine them (Chien, 1998; Verstraete & Van Meirvenne, 2008).

## Methods and approaches

### *WWI war zone and initial dataset*

A study area focusing on the WWI war zone around Ypres, Belgium, was delineated to select the locations of additional soil samples. In comparison with the study area of Van Meirvenne *et al*. (2008), which consisted of the whole province of West-Flanders (3144 km$^2$), a smaller study area of 640 km$^2$ was used for this more detailed inventory. The delineation of our study area was based on the final Cu map of Van Meirvenne *et al*. (2008) (Figure 1). We focused on Cu values exceeding the official background threshold value of 17 mg kg$^{-1}$ soil (DM), as defined by the Flemish Government (Vlaamse Gemeenschap, 1996).

The soil in the war zone consists of Pleistocene wind-blown sediments deposited over Tertiary marine sediments. The topsoil texture is mainly sandy-silt and changes gradually to silt in a north to south direction. The topography is weakly undulating with elevations mostly between 10 and 30 m. A chain of hills, in which the Kemmelberg is the highest (151 m), occurs to the southwest of Ypres.

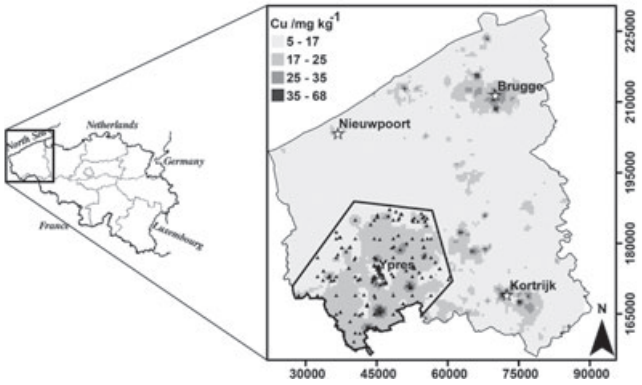


**Figure 1** Belgium with West-Flanders indicated (left), and West-Flanders with the study area indicated (right). The initial dataset (267 locations) is shown on the final Cu map taken from Van Meirvenne *et al*. (2008).

Initially, 267 topsoil (0–50 cm) observations (Figure 1) were available from a geographical database maintained by the Public Flemish Waste Agency (OVAM) and from a study in 1998 by Ghent University (Tack *et al*., 2005). The procedure to determine the total Cu, Pb and Zn concentrations involved a microwave destruction of 0.5 g of the air-dry fine-earth fraction (<2 mm) of soil with HCl, $HNO_3$ and HF acids (OVAM, 1992, CMA/2/II/A.3) and the metals in the digest were analysed by ICP-AES (OVAM, 1992, CMA/2/I/B.1). The OVAM samples were from a single auger hole, while the Ghent University data refer to composite samples from four to eight auger holes.

The OVAM data were collected in the framework of soil pollution investigation according to standard procedures and were analysed for eight heavy metals, among other substances. This means that outliers in the OVAM dataset could have been caused by local soil pollution. Therefore, an intensive clean-up of the data was performed. After the removal of the marginal and spatial outliers (Meklit *et al*., 2009) and the averaging of data pairs with a mutual distance of less than 10 m, 250 data points remained for Cu, 248 for Pb and 247 for Zn.

Table 1 shows the descriptive statistics of the initial dataset. The median for Cu was 2 mg kg$^{-1}$ (values are expressed on a DM soil basis throughout) smaller than was predicted by Van Meirvenne *et al*. (2008); this can be explained by the larger study

**Table 1** Descriptive statistics of the initial dataset of Cu, Pb and Zn / mg kg$^{-1}$ soil (DM)

| | Cu | Pb | Zn |
|---|---|---|---|
| No of data | 250 | 248 | 247 |
| Minimum | 4.5 | 1.0 | 6.7 |
| Median | 16 | 30 | 56 |
| Maximum | 120 | 300 | 520 |
| Mean | 22.0 | 43.9 | 77.3 |
| Variance | 376 | 2109 | 4999 |
| Coefficient of variation | 0.88 | 1.04 | 0.91 |
| Skewness | 2.62 | 2.77 | 3.12 |

 

area. There was a large difference between the mean and median of all three variables, which were positively skewed. The coefficients of variation show that the three datasets had a considerable degree of variation. Although the data were strongly clustered (Figure 1), in a cell declustering analysis (Goovaerts, 1997) the estimated mean fluctuated only slightly with increasing cell size, indicating that there was no preferential sampling towards larger or smaller values in the clusters.

OVAM provided the means to take 300 additional soil samples, of which one-third was intended to be used as an independent validation dataset. The samples were analysed in the same way as the 267 initial samples, but the additional samples were all composites from five auger samplings (0–30 cm) within a radius of 5 m. To constrain the logistic costs we opted for a two-phase sampling strategy with each phase consisting of 100 samples.

## Results and discussion

### *Geostatistical multiphase inventory strategy*

*Phase 1: Selection based on the data configuration.* Because of the clustered configuration of the initial data locations, the first objective was to target the under-represented areas. For this selection we used the Cu dataset because all datasets were very similar for the three metals. As the initial data were strongly skewed, we transformed the data to natural logarithms.

When we applied ordinary point kriging to the log-transformed data on Cu (lognormal ordinary kriging or LOK) on a 200-m square grid using a search window with a radius of 2000 m, which was about the range of the variogram (Van Meirvenne *et al.*, 2008), almost a third of the interpolation points at which kriged estimates were computed had fewer than two neighbours. Therefore, in a first step, 66 locations were randomly selected from among these interpolation points with the condition that the minimum distance between any two of the 66 locations was above 2000 m (Figure 2a). This procedure, with this number of locations, ensured that further predictions at nearly every location could be made from at least two neighbouring data points inside a search-window with a radius of 2000 m. In a second step, we computed the LOK-variance ($\sigma^2_{\mathrm{LOK}}$) at location $\mathbf{x}_0$, i.e. the OK-variance of the log-transformed variable:

$$\sigma^2_{\mathrm{LOK}}(\mathbf{x}_0) = \sum_{\alpha=1}^{N} \{\lambda_\alpha \gamma(\mathbf{x}_\alpha - \mathbf{x}_0)\} + \Psi(\mathbf{x}_0), \qquad (1)$$

where $\lambda_\alpha$ are the weights obtained by solving the OK kriging system of the log-transformed Cu data, $\gamma(\mathbf{x}_\alpha - \mathbf{x}_0)$ are the variogram values for the lag distances between the data points at location $\mathbf{x}_\alpha$, and $\mathbf{x}_0$, obtained after log-transformation of Cu, and $\Psi(\mathbf{x}_0)$ is the Lagrange multiplier.

Because the ordinary kriging variance does not depend on the data values, we included the 66 locations with the initial dataset to compute the $\sigma^2_{\mathrm{LOK}}$ (using the variogram from the initial dataset). The 34 prediction locations with the largest $\sigma^2_{\mathrm{LOK}}$ were then added to the set for further sampling, subject to the condition that no two observations among these additional ones were less than 2000 m apart (Figure 2b). It should be mentioned that in this phase extra samples located outside the study area were used to calculate $\sigma^2_{\mathrm{LOK}}$. Otherwise, the 34 locations would have been selected at the boundaries of the war zone, while our objective

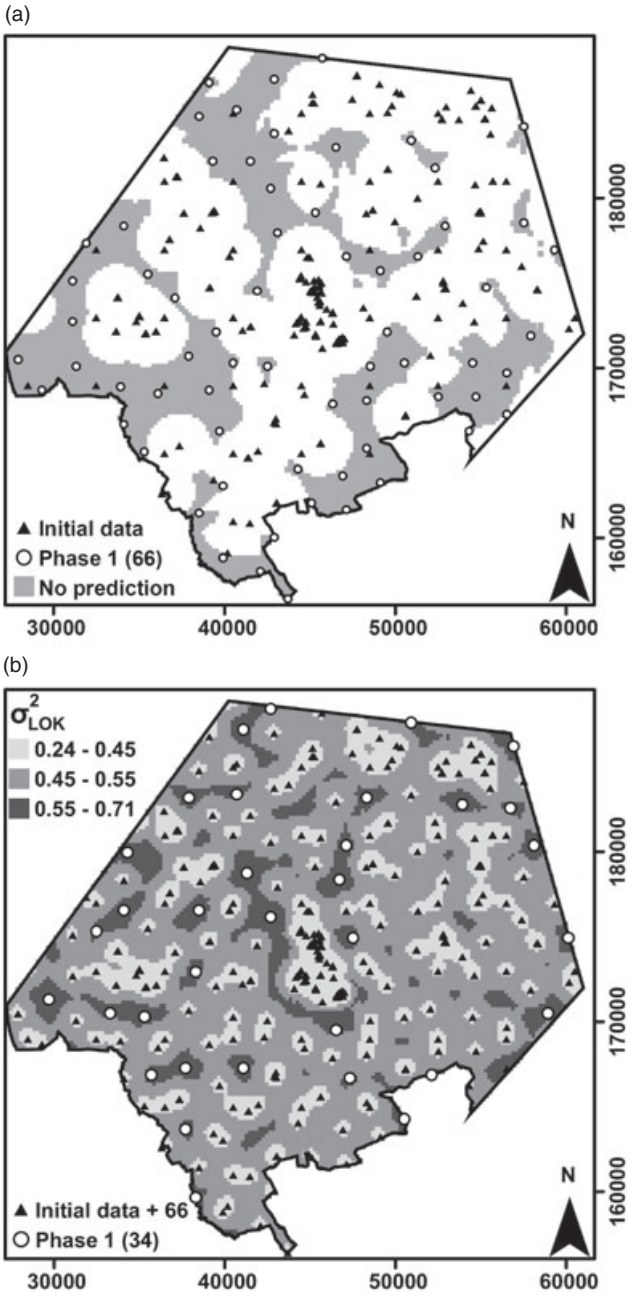


**Figure 2** Selection of the locations during the first sampling phase based on the data configuration of Cu with (a) the 66 locations selected where it was not possible to find two or more data within a search window with a radius of 2000 m, and (b) the 34 locations selected where the $\sigma^2_{\mathrm{LOK}}$ was largest.

 

was to increase the level of detail inside the study area. The samples outside our study area were available from Van Meirvenne *et al*. (2008).

During the actual sampling campaign, one location was inaccessible and could not be sampled. The 99 soil samples obtained were analysed for Cu, Pb and Zn using the same sample support and analytical methods as detailed above.

*Phase 2: Selection based on the data values.* In a second phase, interpolation points with the largest local uncertainty were targeted. This could be assessed by either the conditional variance ($\sigma_C^2$) or the conditional coefficient of variation ($CV_C$). For such log-normal variables, locations with large $\sigma_C^2$ are expected to have large concentrations. However, the $CV_C$ is not expected to be correlated with the mean. Therefore we decided to select equal numbers of locations with large $\sigma_C^2$ and with large $CV_C$. Because both parameters are dependent on the data values, all three metals were considered.

The cdfs required for these parameters were modelled by applying a sequential Gaussian simulation (sGs). The sGs algorithm is described in detail by Webster & Oliver (2007) and Fagroud & Van Meirvenne (2002) provided a flowchart. First, the original data had to be transformed to normal scores, and here the normal score transformations of tied values were adapted to the local average (Saito & Goovaerts, 2000). Then, based on the normal score variogram, sGs was used to generate a number of realizations of the normal scores, which were then back-transformed to the original units. Each realization reproduced the spatial variability of the variable $Z$. Differences between realizations provided a measure of the spatial uncertainty of $Z$, which is a reasonable numerical approximation of the ccdf $[F(Z(\mathbf{x}_0); z|(n))]$, where $|(n)$ represents the conditioning to local information. The simulated values at each location can also be summarized in the local mean (E-type estimate) or local median (M-type estimate). Two software packages were used for the sGs algorithm: the normal score transformation was performed with TerraSeer STIS (Jacquez *et al*., 2005) while SGeMS (Remy *et al*., 2009) was used for the actual simulations.

Using the modelled ccdf, the $\sigma_C^2$ at location $\mathbf{x}_0$ was calculated as

$$\sigma_C^2(\mathbf{x}_0) = \int_0^{+\infty} \{z - z_E^*(\mathbf{x}_0)\}^2 f(Z(\mathbf{x}_0); z|(n))dz, \qquad (2)$$

where $f(Z(\mathbf{x}_0); z|(n))$ is the conditional probability distribution function of $Z(\mathbf{x})$ and $z_E^*(\mathbf{x}_0)$ is the E-type estimate of the variable $Z(\mathbf{x})$ at location $\mathbf{x}_0$. The relative uncertainty as expressed by the $CV_C$ is calculated as

$$CV_C(\mathbf{x}_0) = \frac{\sqrt{\sigma_C^2(\mathbf{x}_0)}}{z_E^*(\mathbf{x}_0)}. \qquad (3)$$

The data used for sGs consisted of the initial dataset plus the samples obtained after phase 1. For each metal, the 16 locations with the largest $\sigma_C^2$ were selected as well as the 16 locations with the largest $CV_C$, resulting in 96 locations. Where there was an overlap between two (or more) of the six sets of 16 locations, an alternative location was selected using the criterion for which the data point was ranked the smallest. For each set of 16 selected locations, we stated as a condition that the minimum distance between the 16 locations was more than 1000 m, according to the obtained normal score variogram ranges (for Cu, Pb and Zn, not shown here). Figure 3 shows the 32 locations selected for Cu during the second sampling campaign.

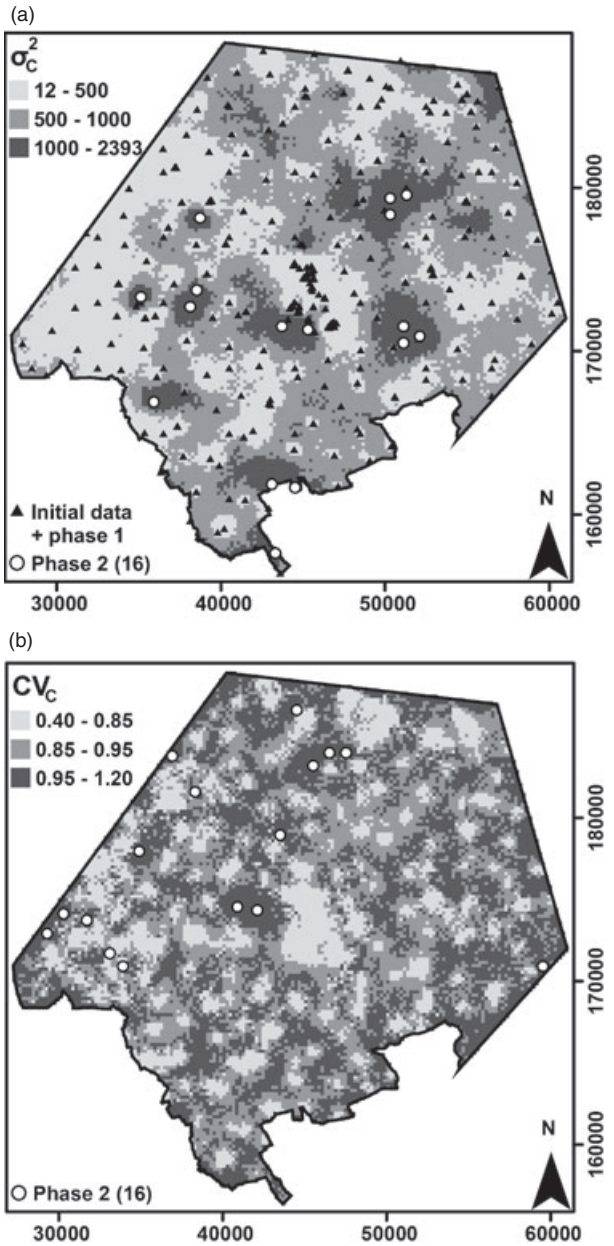


**Figure 3** Selection of the locations for the second sampling phase based on the data values of Cu with (a) the 16 locations using $\sigma_C^2$ and (b) the 16 locations using $CV_C$ as selection criteria.

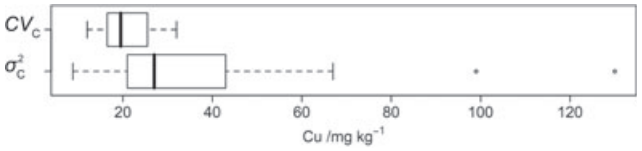


**Figure 4** Boxplots of the 16 Cu concentrations measured at locations using $CV_C$ (top line) and using $\sigma_C^2$ (bottom line) as selection criteria.

At four points sampled in the first phase, concentrations greater than the soil sanitation threshold were measured. Those locations were resampled in addition to the 96 selected locations. Thus in the second sampling phase, a total of 100 locations were sampled and analysed for Cu, Pb and Zn.

Figure 4 illustrates the different consequences of sampling locations with the largest $CV_C$ or the largest $\sigma_C^2$. Two boxplots are shown: one for the 16 Cu concentrations measured at locations selected by the $CV_C$ and another for the 16 Cu concentrations selected by the $\sigma_C^2$. The second boxplot is much wider and contains larger values. In addition, two outliers were measured at locations selected according to $\sigma_C^2$. For Pb and Zn, similar graphs were obtained. The two selection criteria were therefore complementary.

An overview of the data configuration after each phase is given in Figure 5. After the two-phase sampling strategy was performed, each phase was evaluated in terms of prediction accuracy and local uncertainty. Three datasets were used for this evaluation: the initial, the initial + phase 1 and the initial + phase 1 + phase 2.

### *Validation*

*Validation dataset.* The independent validation dataset consisted of 102 data points sampled according to a grid with a cell size of 2412 m by 2490 m. The cell size of the grid was calculated by dividing the range of the $x$ and $y$ coordinates by 11. Because of its irregular shape, 102 of the 121 grid nodes were situated inside the study area. Those data points were used in a jackknife validation to evaluate the improvement of the prediction quality during the data collection.

*Bias and accuracy.* After each step, maps of the median of the ccdfs obtained with sGs of Cu, Pb and Zn were made. Several indices were calculated using the validation dataset: the Pearson correlation coefficient ($r$) between the log-transformed data points

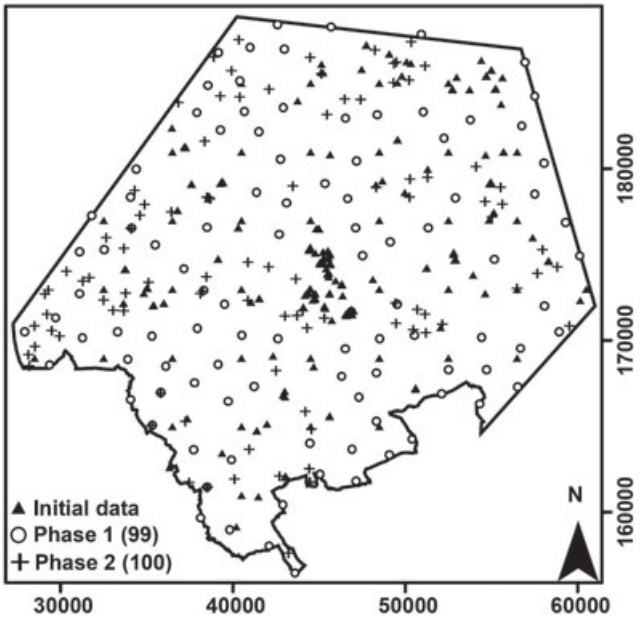


**Figure 5** Summary of the data collection phases.

$z(\mathbf{x}_\alpha)$ and the log-transformed estimates $z^*(\mathbf{x}_\alpha)$, the more robust Spearman rank correlation coefficient ($r_R$), the mean estimation error (MEE) and the root mean square estimation error (RMSEE):

$$\text{MEE} = \frac{1}{n}\sum_{\alpha=1}^{n}(z^*(\mathbf{x}_\alpha) - z(\mathbf{x}_\alpha)), \tag{4}$$

$$\text{RMSEE} = \sqrt{\frac{1}{n}\sum_{\alpha=1}^{n}(z^*(\mathbf{x}_\alpha) - z(\mathbf{x}_\alpha))^2}. \tag{5}$$

The bias of the prediction is indicated by the MEE, while the RMSEE primarily indicates the precision of the predictions. Table 2 lists these statistics for Cu, Pb and Zn. A similar trend was observed for each validation index on each metal in successive phases of the sampling: at each phase the validation index improved and for each metal the largest improvement was obtained after phase 1. In terms of the robust $r_R$, the best results were obtained for Pb; in terms of the MEE (relative to the mean of the validation dataset) Zn scored best. Using the RMSEE, a relative improvement from the initial dataset to the dataset after

**Table 2** Validation indices for Cu, Pb and Zn obtained after each sampling phase with $r$ = Pearson correlation coefficient, $r_R$ = Spearman rank correlation coefficient, MEE = mean estimation error and RMSEE = root mean square estimation error

| | Cu | | | Pb | | | Zn | | |
|---|---|---|---|---|---|---|---|---|---|
| | Initial | After phase 1 | After phase 2 | Initial | After phase 1 | After phase 2 | Initial | After phase 1 | After phase 2 |
| $r$ | −0.08 | 0.20 | 0.27 | 0.06 | 0.30 | 0.37 | 0.11 | 0.18 | 0.22 |
| $r_R$ | 0.09 | 0.29 | 0.33 | 0.10 | 0.32 | 0.35 | 0.16 | 0.23 | 0.29 |
| MEE | −5.5 | −5.1 | −4.5 | −14.6 | −12.5 | −11.4 | −11.6 | −11.6 | −10.5 |
| RMSEE | 26.6 | 25.7 | 25.3 | 75.6 | 73.9 | 72.7 | 68.3 | 67.6 | 67.2 |

 

phase 2 was obtained: Cu improved by 4.9%, Pb by 3.8%, and Zn by 1.6%.

*Local uncertainty.* Another suitable measure to evaluate the improvement of the predictions throughout the data collection is the local uncertainty or the uncertainty about the prediction at a particular unsampled location, $\mathbf{x}_0$ (Goovaerts, 2001). The local uncertainty can be expressed by $\sigma_C^2$ and by $CV_C$. Note that both parameters have already been used as selection critera.

Verstraete & Van Meirvenne (2008) indicated that the average of the coefficient of variation, $\overline{CV_C}$, and the median of the conditional variance, me($\sigma_C^2$), were the best evaluation measures. For instance, for Cu the $\overline{CV_C}$ decreased from 0.925 to 0.912 after the first phase to 0.831 after the second phase, resulting in an overall drop of 10.1%, while the me($\sigma_C^2$) decreased from 640 to 567 after the first phase to 438 after the second phase, resulting in an overall drop of 31.5%. Both parameters improved most when adding the data from the second sampling phase, in contrast to the change in the local validation parameters. This can be explained by the intention of the second sampling phase to decrease the local uncertainty.

More interesting is the analysis of the change in the spatial distribution of the local uncertainty throughout the data collection. Figure 6 shows the maps of the predicted $CV_C$s for Cu created by sGs based on 250 (Figure 6a) and 449 data points (Figure 6b). Figure 6(a) reflects the unequal spread of the initial data points. It is clear that with increasing size of the datasets, the $CV_C$ generally decreases and the map becomes more homogeneous (Figure 6b). In particular, adding the 100 samples from phase 2 caused a substantial improvement, both on the $CV_C$ map and on the average $CV_C$. These conclusions for Cu are also valid for Pb and Zn.

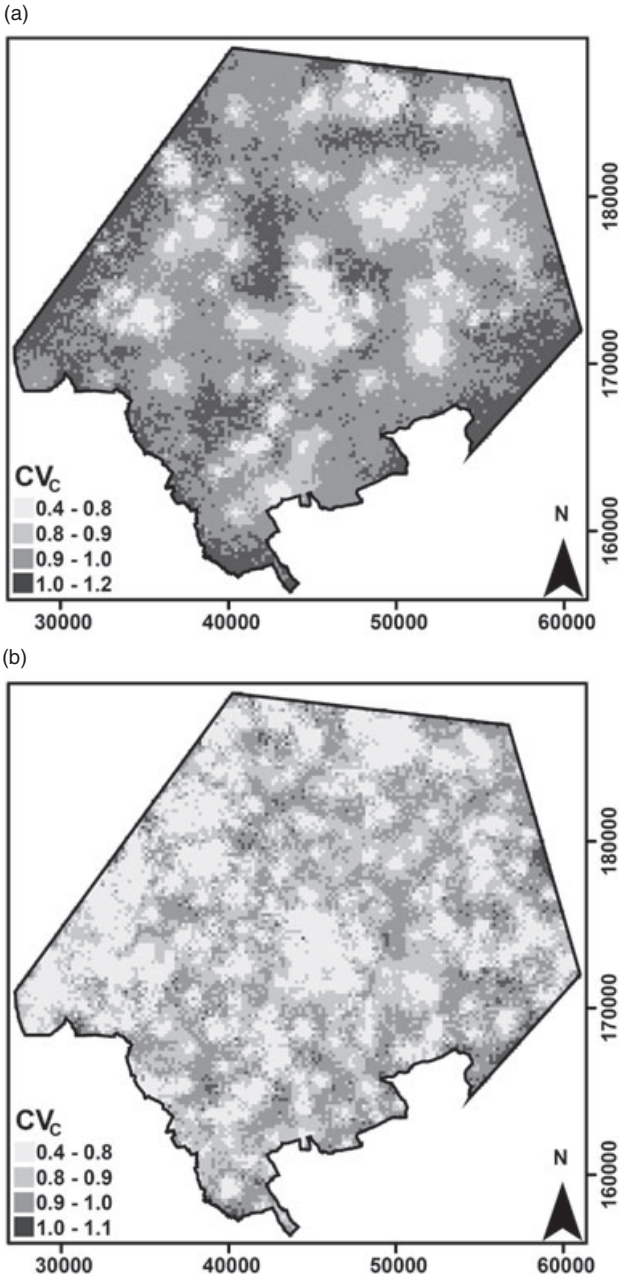


**Figure 6** The conditional coefficient of variation ($CV_C$) calculated based on (a) the 250 initial Cu data and (b) the 449 Cu data after sampling phase 2.

### *Inventory of Cu, Zn and Pb*

To create the final maps we used all available data: the dataset obtained after the second sampling phase and the validation data. The final maps for Cu, Pb and Zn were therefore based on 551, 548 and 548 data points, respectively. The extreme Pb concentration of 7600 mg kg$^{-1}$ soil, sampled during the first phase, was not considered.

The descriptive statistics of the final dataset can be found in Table 3. Because of the addition of larger values, the skewness of the three variables increased considerably. The median for Cu increased from 16 to 18.6 mg kg$^{-1}$. The Cu mean value increased slightly during the data collection, while the Pb mean and median values remained steady. The Zn median increased by 1.9 mg kg$^{-1}$, whereas the mean decreased by 4.9 mg kg$^{-1}$. The increase in the Pb coefficient of variation was particularly marked.

Figure 7 shows the experimental variograms, $\gamma(\mathbf{h})$, and their models for the normal score-transformed data points of Cu, Pb and Zn. The variogram parameters can be found in Table 4, with $C_0$ the nugget variance, $C_0 + C_1$ the sill and $a$ the range. The variogram models for Cu and Pb were spherical whereas that for Zn was exponential. For Cu and Pb a similar range was found (around 1600 m), while for Zn the range was smaller (1198 m). The nugget-to-sill ratio (NSR) was small for Cu (0.345) and increased to 0.442 for Pb and to 0.541 for Zn.

The final predictions were obtained by using the median estimate of the ccdfs generated by sGs with a resolution of 200 m by 200 m and a search window with a radius of 5000 m (Figure 8). When comparing our Cu map (Figure 8a) with the final prediction map of Van Meirvenne *et al*. (2008) (Figure 1), some

**Table 3** Descriptive statistics of the final dataset (including validation data) of Cu, Pb and Zn/mg $kg^{-1}$ soil (DM)

| | Cu | Pb | Zn |
|---|---|---|---|
| No of data | 551 | 548 | 548 |
| Minimum | 4.5 | 1.0 | 6.7 |
| Median | 18.6 | 30 | 58 |
| Maximum | 250 | 950 | 620 |
| Mean | 22.8 | 44.0 | 72.4 |
| Variance | 404.8 | 3704 | 3315 |
| Coefficient of variation | 0.88 | 2.67 | 0.80 |
| Skewness | 4.97 | 9.15 | 4.59 |

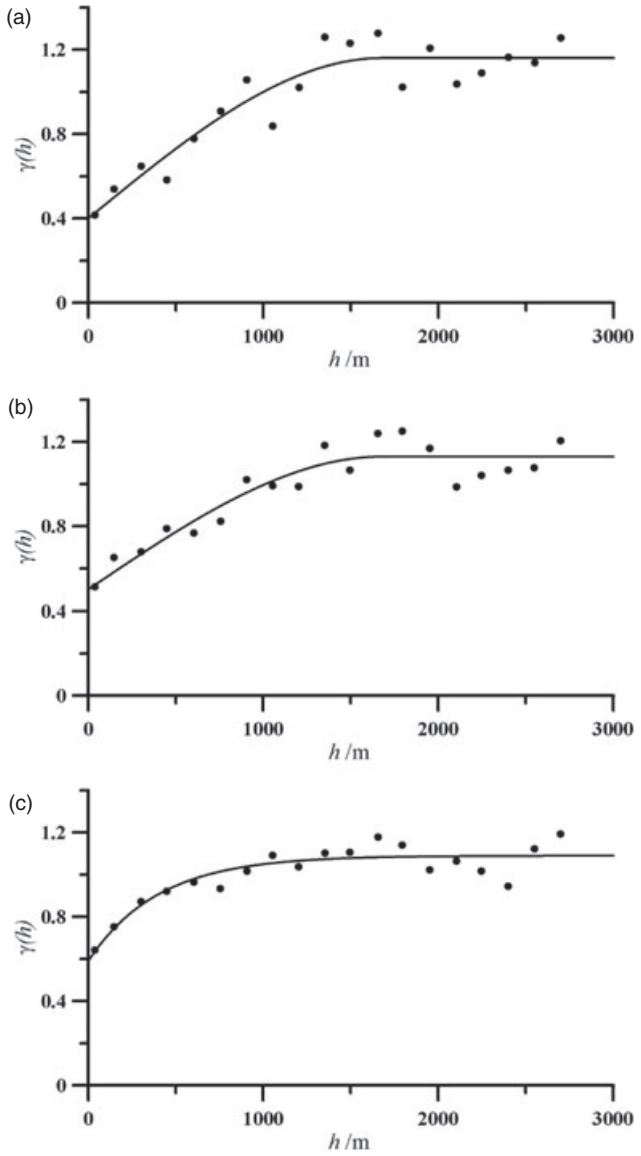


**Figure 7** Experimental variograms (points) and variogram models (curves) of the final (a) Cu, (b) Pb and (c) Zn data.

**Table 4** Parameters of the variogram models fitted to the experimental variograms of the normal scores of the final dataset, including the validation data, of Cu, Pb and Zn, with $C_0$ the nugget variance, $C_0 + C_1$ the sill and $a$ the range. The NSR is the nugget-to-sill ratio

| Type | Cu Spherical | Pb Spherical | Zn Exponential |
|---|---|---|---|
| $C_0$ | 0.40 | 0.50 | 0.59 |
| $C_1$ | 0.76 | 0.63 | 0.50 |
| $a$ / m | 1674 | 1682 | 1198 |
| NSR | 0.345 | 0.442 | 0.541 |

changes can be observed. A hotspot appeared in the southeast of the Cu map of Van Meirvenne *et al.* (2008), where a large Cu concentration was associated with a car assembly site. While Van Meirvenne *et al.* (2008) only masked the large values caused by industrial activities during variogram modelling, we removed such values entirely during the data clean-up. In our Cu map, an area with clearly observable large values appeared to the east of Ypres. During WWI intensive fighting took place in this area and well-known sites such as Hill 60, Hill 62 and Geluveld are located there. The Pb map (Figure 8b) shows an analogous pattern with the same hotspot east of Ypres. The pattern of the Pb enrichment corresponds to the front line. The Zn map (Figure 8c) on the other hand is characterized by a different pattern; the largest concentrations were not linked with the frontline. This could be explained by the relatively small amount of Zn in shells and by the greater mobility of Zn in soils.

## Conclusions

We have demonstrated a two-phase sampling strategy aimed at increasing the detail of an inventory, rather than delineating a contaminated area with respect to a critical threshold. In the case of an initial dataset that is strongly clustered sampling in less densely sampled regions should be the first objective. Therefore, selection criteria based on the ordinary kriging variance or distance measures can be used. After filling the spatial gaps, focusing on the local uncertainty is advisable. For this purpose, both the conditional variance and the conditional coefficient of variation are suitable and complementary selection criteria. A clear improvement of four validation indices demonstrated the benefits of our data collection. It was concluded that an appropriate combination of geostatistical selection criteria is the key to an efficient sampling campaign.

Further research could focus on investigating whether the selection criteria based on $\sigma_C^2$ and $CV_C$ should be treated equally and on defining multiple objective criteria in which the three metals are considered simultaneously. The expansion of the dataset to include other metals revealed that both Cu and Pb showed analogous patterns related to WWI activities. Increased concentrations of Cu and Pb were found in areas where intensive fighting took place during WWI, whereas for Zn no apparent relationship with WWI activities could be seen.

 

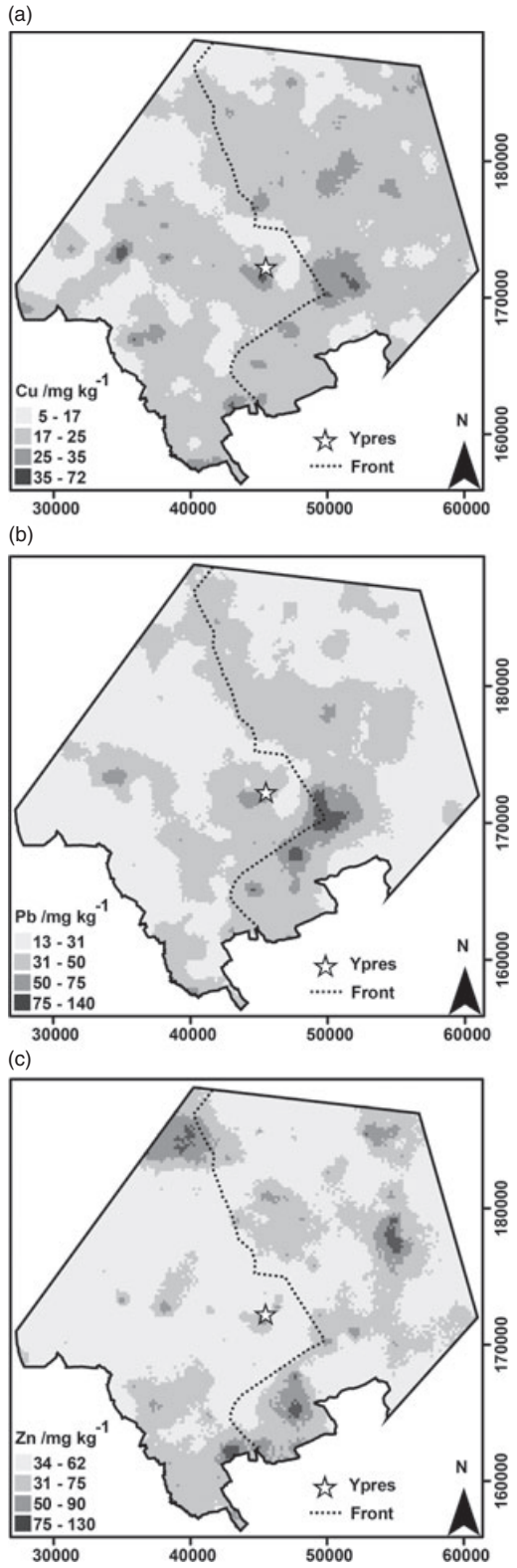


**Figure 8** Prediction maps for the topsoil (a) Cu, (b) Pb and (c) Zn content obtained by sequential Gaussian simulation (using the median) with the centre of Ypres indicated and the frontline, which remained more or less stable between 1915 and 1917 (Chielens *et al*., 2006).

## Acknowledgements

The authors thank OVAM for financing the sampling campaign and providing data on heavy metals in the soil of Flanders. Alain Coopman and Kurt Bouckenooghe (Soresma nv) are kindly thanked for performing the sampling campaign. We also thank Professor F. Tack for allowing us to use some additional heavy metal data and Meklit Tariku Chernet for the interesting scientific discussions. We gratefully acknowledge the financial support of the Flemish Fund for Scientific Research (Aspirant FWO-Vlaanderen).

## References

Barabás, N., Goovaerts, P. & Adriaens, P. 2001. Geostatistical assessment and validation of uncertainty for three-dimensional dioxin data from sediments in an estuarine river. *Environmental Science & Technology*, **35,** 3294–3301.

Burgess, T.M., Webster, R. & McBratney, A.B. 1981. Optimal interpolation and isarithmic mapping of soil properties: IV. Sampling strategy. *Journal of Soil Science*, **31,** 315–331.

Chielens, P., Dendooven, D. & Decoodt, H. 2006. *De laatste getuige: het oorlogslandschap van de Westhoek.* Uitgeverij Lannoo nv, Tielt.

Chien, Y.J. 1998. *A Geostatistical Approach to Sampling Design for Contaminated Site Characterization*. Master thesis, Stanford University, Stanford, CA.

D'Or, D. 2005. Towards a real-time multi-phase sampling strategy optimization. In: *geoENV V – Geostatistics for Environmental Applications* (eds P. Renard, H. Demougeot-Renard & R. Froidevaux), pp. 355–366. Springer-Verlag, Berlin.

Englund, E.J. & Heravi, N. 1994. Phased sampling for soil remediation. *Environmental & Ecological Statistics*, **1,** 247–263.

Fagroud, M. & Van Meirvenne, M. 2002. Accounting for soil spatial autocorrelation in the design of experimental trials. *Soil Science Society of America Journal*, **66,** 1134–1142.

Garcia, M. & Froidevaux, R. 1997. Application of geostatistics to 3-D modelling of contaminated sites: a case-study. In: *geoENV I – Geostatistics for Environmental Applications* (ed. A. Soares), pp. 309–325. Kluwer Academic Publishing, Dordrecht.

Goovaerts, P. 1997. *Geostatistics for Natural Resources Evaluation.* Oxford University Press, New York.

Goovaerts, P. 2001. Geostatistical modelling of uncertainty in soil science. *Geoderma*, **103,** 3–26.

Jacquez, G.M., Greiling, D.A. & Kaufmann, A.M. 2005. Design and implementation of a Space-Time Intelligence System for disease surveillance. *Journal of Geographical Systems*, **7,** 7–23.

Lloyd, C.D. & Atkinson, P.M. 1999. Designing optimal sampling configurations with ordinary and indicator kriging. *Proceedings of the 4th International Conference on GeoComputation, 25–28 Jul 1999*, Fredericksburg, VA. Greenwich GeoComputation CD-ROM [WWW document]. URL http://www.geocomputation.org/1999/065/gc_065.htm [accessed in 2009]

Meklit, T., Van Meirvenne, M., Verstraete, S., Bonroy, J. & Tack, F. 2009. Combining marginal and spatial outliers identification to optimize the mapping of the regional geochemical baseline concentration of soil heavy metals. *Geoderma*, **148,** 413–420.

OVAM 1992. *Compendium voor monsterneming en analyse ter uitvoering van het afvalstoffendecreet en het bodemsaneringsdecreet.* Openbare Afvalstoffenmaatschappij voor het Vlaamse Gewest, Mechelen.

Pardo-Igúzquiza, E. & Dowd, P.A. 2005. Multiple indicator cokriging with application to optimal sampling for environmental monitoring. *Computers & Geosciences*, **31,** 1–13.

Remy, N., Boucher, A. & Wu, J. 2009. *Applied Geostatistics with SGeMS. A User's Guide.* Cambridge University Press, New York.

Saito, H. & Goovaerts, P. 2000. Geostatistical interpolation of positively skewed and censored data in a dioxin-contaminated site. *Environmental Science & Technology*, **34,** 4228–4235.

Tack, F.M.G., Vanhaesebroeck, T., Verloo, M.G., Van Rompaey, K. & Van Ranst, E. 2005. Mercury baseline levels in Flemish soils (Belgium). *Environmental Pollution*, **134,** 173–179.

Van Groenigen, J.W. & Stein, A. 1998. Constrained optimization of spatial sampling using continuous simulated annealing. *Journal of Environmental Quality*, **27,** 1078–1086.

Van Meirvenne, M. & Goovaerts, P. 2001. Evaluating the probability of exceeding a site-specific soil cadmium contamination threshold. *Geoderma*, **102,** 75–100.

Van Meirvenne, M., Meklit, T., Verstraete, S., De Boever, M. & Tack, F. 2008. Could shelling in the First World War have increased copper concentrations in the soil around Ypres? *European Journal of Soil Science*, **59,** 372–379.

Verstraete, S. & Van Meirvenne, M. 2008. A multi-stage sampling strategy for the delineation of soil pollution in a contaminated brownfield. *Environmental Pollution*, **154,** 184–191.

Vlaamse Gemeenschap 1996. *Besluit van de Vlaamse regering houdende vaststelling van het Vlaams reglement betreffende de bodemsanering*. Belgisch staatsblad of 27 March 1996, Brussels.

Webster, R. & Burgess, T.M. 1984. Sampling and bulking strategies for estimating soil properties of small regions. *Journal of Soil Science*, **35,** 127–140.

Webster, R. & Oliver, M.A. 2007. *Geostatistics for Environmental Scientists*, 2nd edn. John Wiley & Sons, Chichester.

 